Polymer 232 (2021) 124167

Contents lists available at ScienceDirect

Polymer

journal homepage: www.elsevier.com/locate/polymer

Influence of the rosin pendant groups on the solution properties of a high molecular weight hydrogenated polynorbornene

Nasrollah Hamidi [a,*], Mitra Shiran Ganewatta [b]

[a] Department of Biological and Physical Sciences, South Carolina State University, Orangeburg, SC 29115, USA
[b] Department of Chemistry and Biochemistry, University of South Carolina, Columbia, SC, 29208, USA

ARTICLE INFO

Keywords:
Polynorbornene
Rosin
Viscosity
Flexibility
Mark-houwink
Stockmayer-Fixman
Touched-bead model

ABSTRACT

The dilute solution properties of a sample of high molecular weight rosin substituted hydrogenated polynorbornene (hPDNB) homopolymer, prepared via ROMP and post-polymerization modified by backbone hydrogenation, was investigated by the online measurement of intrinsic viscosity, refractive index, two-angle light scattering and size exclusion chromatography (SEC) in tetrahydrofuran (THF) at 35 °C. The weight average molecular weight ($\overline{M}_w$), intrinsic viscosity ([η]), radii of gyration ($\overline{R}_G$) and hydrodynamic ($\overline{R}_H$) radii, and concentration of the polymer fractions were obtained from corresponding traces of the chromatograms. From these data, the double logarithmic plots of $\overline{M}_w$ versus [η], $\overline{M}_w$ versus $\overline{R}_G$ and $\overline{R}_H$, and $[\eta]\overline{M}_w^{-½}$ versus $\overline{M}_w^{½}$ scaled the dimensions of the polymer chains to molar mass. The results, surprisingly, indicated that the rosin-substituted polynorbornene is flexible like poly(methyl acrylate). To confirm the results, the data were analyzed by the worm-like touched-bead model which predicated the polymer to be more rigid than poly(methyl acrylate) but less rigid than hindered poly(di-alkyl phenyl acrylate) and poly(di-tert-butyl fumarate).

1. Introduction

Using natural biomass as raw material resources for polymer development is gaining significant attention [1]. Rosin is the non-volatile material found in the resinous exudate of plants belonging to the conifer family, for example, spruce and pine trees. It is a mixture of diterpenes biosynthesized as a part of their natural defense mechanism against herbivore and pathogen attacks [2]. Rosin consists of several abietic- and pimaric-type isomers called resin acids, which have a tertiary carboxylic acid group, unsaturations, and a bulky hydrophenanthrene ring structure that can increase glass transition temperature and render hydrophobicity to any substrates to which it is attached [3]. Rosin is isolated as gum rosin, wood rosin or tall oil rosin and the annual world production is ~1.2 million tons [4,5]. Rosin derivatives are used commercially as adhesive tackifiers, ink resins, paper sizing, and emulsifiers among other applications. Due to the presence of unique thermo-mechanical properties, rosin derived polymers and composites have gained significant interest in recent controlled polymerization research [4,6]. These materials include poly(meth)acrylates [7], degradable polyesters [8,9], rosin-lignin or cellulose composites [3,10], drug-delivery nanogels [11], and antimicrobial polymers and surfaces [12–14]. The polymer under this study is a rosin-substituted polynorbornene homopolymer prepared via ring-opening metathesis polymerization (ROMP) and post-polymerization modified via polymer backbone hydrogenation [15]. This class of polymers is the first reported high molecular weight rosin-based polymers with molecular weights exceeding the chain entanglement molecular weight of 86 kDa. This strategy as well as related penta-block copolymers prepared via ROMP provide mechanically robust thermoplastics from rosin acids [16]. These ROMP-based synthetic strategies provide a path to overcome the inherent brittleness of rosin-derived polymers.

The influence of pendant groups on the physical properties of polyethylene chains such as the case of low-density polyethylene (LDPE), high-density polyethylene (HDPE), polypropylene (PP), polybutylene (PB) is well documented [17]. In the case of poly(meth)acrylates, interest has been focused on the changes induced by altering the length of the alkyl ester group [18] or identity of the ester linkage such as phenyl with alkyl substituent in various positions [19]. In the case of polycaprolactone (PCL), the researchers focused on evaluating the effects of grafting a bulky group such as dehydroabietic acid as the pendant onto the back-bone of PCL [20].

Exploring the solution properties of rosin-based polymers is essential

* Corresponding author.
E-mail address: nhamidi@scsu.edu (N. Hamidi).

https://doi.org/10.1016/j.polymer.2021.124167
Received 27 June 2021; Received in revised form 3 September 2021; Accepted 6 September 2021
Available online 7 September 2021
0032-3861/Published by Elsevier Ltd.

for evaluating their utility in advanced materials design. This work presents the influence of the rosin pendant groups on the solution properties of the hydrogenated polynorbornene polymer poly(dehydroabietanyl norborn-5-ene-2-carboxylate) (hPDNB) studied by intrinsic viscosity and molar mass relationship based on Kuhn-Mark-Houwink-Sakurada (MH) [17–25] and Stockmayer-Fixman (S-F) relationships [21]. By the aid of the most common two-parameter theories, MH and S-F relationships, the conformational properties of the polymer including end-to-end distance [$(\overline{R}_0^2)^{1/2}$], rigidity factor (σ), and Flory's characteristic ratio (C_∞) were estimated [17–23]. Since the obtained parameters were not describing the polymer properly, its properties were estimated based on the worm-like touched-bead model [24–29]. We hope this study could shed light on many other types of side-chain modified hydrogenated polynorbornenes.

2. Experimental

2.1. Materials

Standard calibration samples of polystyrene with narrow molecular mass distribution were purchased from Sigma-Aldrich Co. (USA); tetrahydrofuran (THF) was purchased from Thermo-Fisher Scientific (USA). Other solvents and reagents were purchased from the above-mentioned companies and used without further treatment.

2.2. Polymer synthesis

Norbornene and its derivatives can undergo polymerization via ring-opening olefin metathesis, cationic or radical polymerization, and by vinyl or addition polymerization [30]. In contrast to other methods, ROMP retains only a single ring in the repeat unit resulting in polymers with flexible chains. The polymer hPDNB sample was prepared via ROMP of the dehydroabietic acid containing norbornene monomer dehydroabietanyl norborn-5-ene-2-carboxylate (DNB) using Hoveyda-Grubbs Catalyst® 2nd Generation, as outlined in our previous work [15] and here in Scheme 1. This was followed by post-polymerization diimide reduction using p-toluene sulfonyl hydrazide, which resulted in the final product rosin-substituted hydrogenated polynorbornene polymer hPDNB with a saturated backbone and pendant groups derived from dehydroabietic acid.

In our prior work, ^{1}H NMR spectra confirmed the successful preparation and saturation of the polymer backbone resulting in the hPDNB homopolymer, where the degree of hydrogenation was over 97% [15]. The reported DSC data indicated a T_g of 85 °C for hPDNB. In addition, hPDNB is an amorphous polymer unlike typical hydrogenated polynorbornene polymers that show a melting point in the range of 92–134 °C, depending on the hydrogenation method [31]. Our investigation on how the pendant rosin groups influence the hydrogenated polynorbornene backbone is discussed in the following sections.

2.3. Instrumentation

The intrinsic viscosity of the sample and hence its light scattering, and refractive index at various injected volumes were measured by a Viscotek/Malvern (USA) GPC-Max-TDA 302. The GPC was equipped with three Viscogel-I series mixed bed columns (7.8 mm × 30 cm) having 7,500 theoretical plate per column, I-MBLMW-3078 for low molar mass polymers (exclusion limit 20,000 Da, max. pore size 1000 Å), I-MBMMW-3078 for medium molar mass polymers (exclusion limit 200,000 Da, max. pore size 10,000 Å), and I-MBHMW-3078 for higher molar mass polymers (exclusion limit 10,000,000 Da, max. pore size 100,000). The light scattering cell online with GPC-Max-TDA 302 consists of an 18 μL cell with laser light at 760 nm, and two-light scattering detectors, one at the right angle and the other at a low angle (~7°). The GPC-Max-TDA 302 was also equipped with a refractive index deflection type detector with reference cell volume 12 μL and light-emitting diode (LED) at 660 nm wavelength. The viscometer was a four capillary, differential pressure Wheatstone bridge configuration viscometer (DP) with a bridge volume of about 72 μL. The viscometer shear rate at a flow rate of 3.0 mL/min of THF was ~3000 sec^{-1}. The flow rate of hPDNB in THF samples was 0.5 mL/min which results in a lower shear rate than 3000 sec^{-1}.

The solution was prepared gravimetrically by measuring the weight of the solvent and solute using a Mettler-Toledo XS205 Dual-Range analytical balance with an uncertainty of 0.02 mg and the concentrations were evaluated by the corresponding density of the solvent to have higher accuracy and precision. The standard 2 mL clear glass, screw cap vials were filled with 1.8 mL of the sample, then they were placed in the corresponding vial rack number. Four aliquots of the same solution (75, 100, 125, and 150 μL) of hPDNB in THF were prepared a day before use and a sample of standard PS was injected into a fixed 200 μL volume sample loop by GPC-Max auto-sampler. The syringe was washed twice before and after each injection. RI and DP cells were purged 5 min before

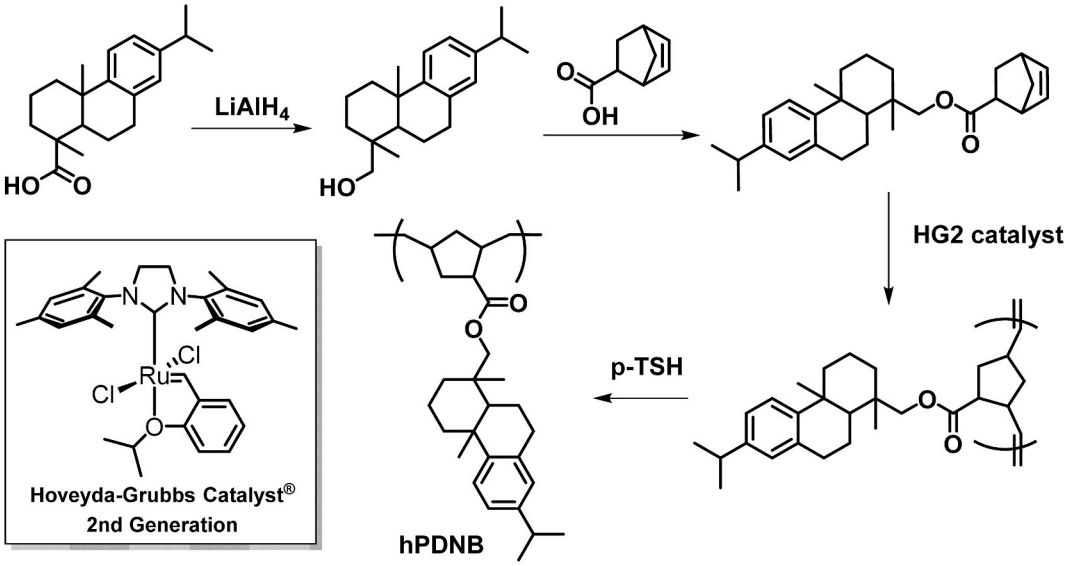

Scheme 1. Synthesis of the rosin-derived norbornene monomer, its polymerization and post-polymerization modification to obtain the rosin-substituted hydrogenated polynorbornene, a high molecular weight homopolymer containing dehydroabietic pendent groups [15].

and after each injection. The GPC-Max-TDA 302 was controlled by Omnisec 4.2 software (Viscotek/Malvern USA) running on a Dell PC. The columns and all detectors were housed in the same thermostated oven.

2.4. Measurements and results

Fig. 1 shows the chromatograms of simultaneous measurements of light scattering, refractive index, and intrinsic viscosity of hPDNB at 35 °C when 100 μL of the solution was injected into the GPC-Max-TDA 302 instrument. The data obtained from four similar chromatograms with variable amounts of polymer (75, 100, 125, and 150 μL) were used for this study. In this method, the molecular weight was available from the light scattering detectors, the intrinsic viscosity was obtained by a differential Wheatstone bridge configuration viscometer, and the concentration of the polymer was obtained by the intensity of the refractive index [32,33].

A polymer sample with a wider range of molecular weight distribution offer fractions of polymers with a wider range of molecular weight and hence the triple detector measurements of these polymers seem like the most elegant way to characterize a polymer in solution. In this case, a single measurement can simultaneously yield several characteristic parameters of a macromolecular sample, including weight-average molecular weight ($\overline{M}_w$), number-average molecular weight ($\overline{M}_n$), dispersity ($Đ_M = \overline{M}_w/\overline{M}_n$), intrinsic viscosity [η], the radius of gyration ($\overline{R}_G$), hydrodynamic radius ($\overline{R}_H$), and *dn/dc* of samples in solution. The dispersity of the polymer sample ($Đ_M$) was estimated to be 1.55.

3. Results and discussion

3.1. Refractive index increment, dn/dc

The *dn/dc* parameter is one of the relevant physical properties of a polymer solution particularly when it is related to the determination of the molecular weight of a polymer by the light scattering method. The value of *dn/dc* indicates the change of refractive index versus concentration of a solution at a given temperature and a given wavelength of light. It can be obtained from the slope of the Eq. (1) using GPC-Max-TDA 302 chromatograms data:

$$n = \frac{dn}{dc} \cdot \frac{RI_{Cal}}{n_0} .C \quad (1)$$

where n and n_0 are the refractive index of solution and pure solvent, respectively; RI_{cal} is the instrument calibration factor of refractive index at a given temperature, and C is the concertation of the polymer in a given trace. Fig. 2 shows the plots of variations of the refractive index of hPDNB solution versus (RI_{cal}/n_0)C; the slope of the plot gives the accurate value of $dn/dc = 0.1233$ dL/g of the sample. Typically, the values of *dn/dc* for most homo-polymers are nearly constant in a wide range of molar mass at a given temperature and solvent, similar to the case of hPDNB in this work, polystyrene in THF [33], polycaprolactone grafted propargyl dehydroabietic ester (PCL-g-DAPE) in THF [34], and poly (α-methylstyrene) in cyclohexane [35].

3.2. Intrinsic viscosity and molecular weight

The widely used relationship between [η] and $\overline{M}_w$ is the Mark-Houwink-Kuhn-Sakurada (MH) relationship [36–38].

$$[\eta] = K_\nu \overline{M}_w^{\nu} \quad (2)$$

where the parameter ν is a measure of the thermodynamic power of the solvent and K_ν is a measure of the coil volume under unperturbed conditions. The [η] of a polymer in a dilute solution is a measure of its hydrodynamic size and conformation [39]. Fig. 3 shows the double logarithmic variation of $\overline{M}_w$ versus [η] for the hPDNB in THF when four different aliquot (75, 100, 125, and 150 μL) of the same solution (1.80 g/L) was injected to the GPC-Max-TDA 302 at 35 °C. With this technique, a sample with $\overline{M}_w = 432$ kDa is fractionated to its corresponding 1,200 traces covering a wide range of molar mass, 145 kDa $< \overline{M}_w <$ 3, 980 kDa. The value of ν depends on the thermodynamics power of the solution and hence it stays constant in a wide range of molar mass. The values of ν and [η] of this system obtained from the MH plot are tabulated in the columns 3 and 4 of Table 1. The values of ν and [η] did not change with the molecular weight of the polymer, hence, there was no conformational transition due to molecular weight of hPDNB in THF in the studied molar mass ranges.

The ν value of 0.705 ± 0.007 (Table 1) of MH's exponent of hPDNB at 35 °C was similar to the ν value of PCL, a flexible polymer at 25° in THF [40,41], and was also in the range of random coil polymers in very good solvents. In a good solvent, the polymer coils are perturbed by the

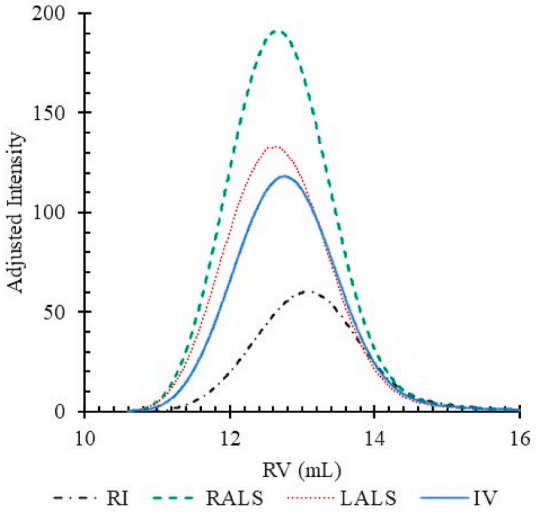

Fig. 1. The chromatogram of the simultaneous measurements of light scatterings (LALS & RALS), refractive index (RI), and intrinsic viscosity (IV) at 35 °C when 100 μL of hPDNB in THF was injected into GPC-Max-TDA 302 system.

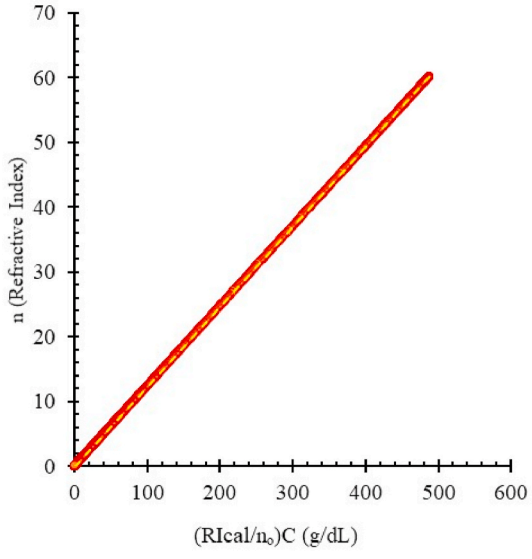

Fig. 2. Variation of the refractive index (n) with adjusted concentration, (RI_{cal}/n_0)C at 35 °C (- - -), where the filled points show the experimental data.

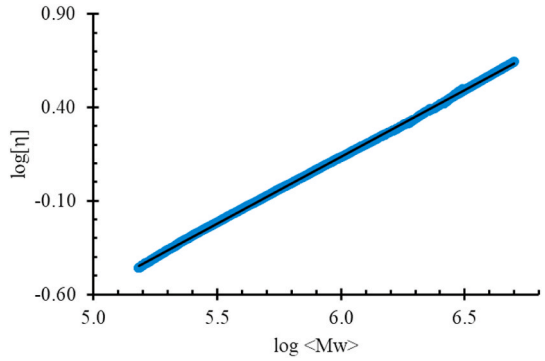

Fig. 3. The double logarithmic plot of [η] (dL/g) vs $\overline{M}_w$ of hPDNB at 35 °C. The filled points show the experimental data.

thermodynamic power of the solvent. In this case, the renormalization group theory predicts a value of $\nu = 0.764$ for an extremely good solvent. However, in practice, smaller values (<0.764) are often found for perturbed coils in good solvents. This kind of behavior is common in cases where some moderately good solvents or branched polymers are studied [26].

3.3. Dependence of $\overline{R}_H$ and $\overline{R}_G$ on the molecular weight of hPDNB

Fig. 4 represents the double logarithmic variation of average hydrodynamic radii ($\overline{R}_H$) and radii of gyration ($\overline{R}_G$) versus $\overline{M}_w$ at temperature 35 °C for the inject volumes of 75, 100, 125, and 150 μL of hPDNB in THF. The values of the values of slope (γ) and Y-intercepts (K_γ) of the logarithmic variation of $\overline{R}_H$ versus $\overline{M}_w$ are tabulated in the 5th and 6th columns of Table 1; and the corresponding values of the logarithmic variation of $\overline{R}_G$ versus $\overline{M}_w$ are tabulated in the 7th and 8th columns of the same Table. For monodispersed rigid spheres, the variation of hydrodynamic radii and radii of gyration are identical. For sufficiently long flexible polymer chains in good solvents, these radii are expected to differ from one another but to vary with molecular weight in the same way as shown in Fig. 4 for hPDNB. In general, both K_γ and γ are functions of the solvent quality and chain dimension as described by Flory [17], Yamak and many others [35,42]. For flexible polymers, the values of $\overline{R}_H$ and $\overline{R}_G$ are proportional to $\overline{M}_w^{1/2}$ at the θ-condition. In a good solvent, the polymer coil volume expands, thus the relationship mimicking the form of the variation of intrinsic viscosities by molecular weight as:

$$\overline{R}_H = k_{\gamma H}\overline{M}_w^{\gamma H} \tag{3A}$$

$$\overline{R}_G = k_{\gamma G}\overline{M}_w^{\gamma G} \tag{3B}$$

For hPDNB in THF at 35 °C, $\gamma_H = 0.567 \pm 0.002$ (Table 1, 5th column), is within the obtained $\gamma_G = 0.564 \pm 0.003$ (Table 1, 7th column). These values indicates that the $\overline{R}_H$ and $\overline{R}_G$ vary similar as was expected and are within the predicted value for a random coil polymer in a moderately good solvent.

3.4. Evaluation of unperturbed dimension

In a very good solvent, such as the case of hPDNB in THF at 35 °C, the unperturbed dimension and hence the fundamental conformational characteristic of the polymer, $(\overline{R}_0^2/M)^{1/2}$ (fifth column of Table 2) was obtained by using Stockmayer-Fixman (S-F) [21] extrapolation method (Fig. 6A). This semi-theoretical relationship relates the excluded volume equation to the molecular weight and intrinsic viscosity of homologs series of polymers, the final equation comes as:

$$[\eta]\overline{M}_w^{1/2} = K_\theta + 0.346\Phi_0 B\overline{M}_w^{1/2}\,; 0 \le \alpha^3 \le 1.6 \tag{4}$$

Where B relates to the polymer-solvent interaction energy and Φ_0 is Flory's universal viscosity constant. Its value vary depending on the nature of the polymer sample and its molecular weigh distribution [43]. In this work, we used the recommended value of 2.7×10^{23} mol^{-1} (cgs) when [η] expressed in mL/g to evaluate the characteristics of hPDNB, which are tabulated in Table 3 [36,37]. K_θ, is the Y-intercept of the S-F plot, which is related to the unperturbed dimensions of the polymer y Eq. (5):

$$\left(\frac{\overline{R}_0^2}{\overline{M}_w}\right)^{1/2} = \left(\frac{K_\theta}{\Phi_0}\right)^{1/3} \tag{5}$$

The expansion of a polymeric chain in a stronger solvent expressed

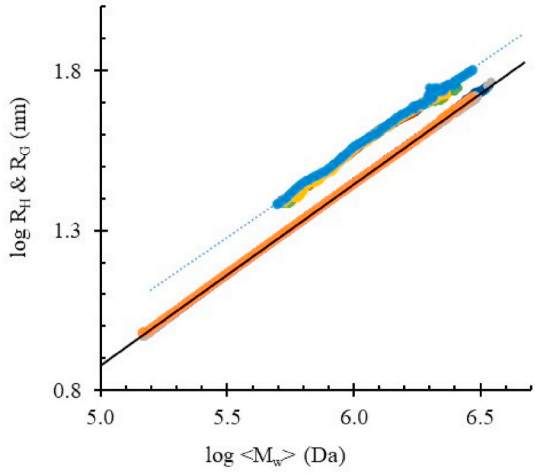

Fig. 4. Hydrodynamic radii (—) and radii of gyration (… …) as a function of molecular weight for the hPDNB in THF at 35 °C. The filled points show the experimental data.

Table 1
MH parameters (ν and K_ν), hydrodynamic radius, and radius of gyration of hPDNB in THF at 35 °C. Polycaprolactone (PCL), PCL grafted propargyl dehydroabietic ester (PCL-g-DAPE), atactic polypropylene (aPP), poly(methyl acrylate) (PMA), poly(diisopropyl fumarate) (PDiPF), and poly(3,5-dimethyl-phenyl acrylate) (35PDMPA) are included for comparison.

Experiment	T (°C)	MH (mL/g)			R_H		R_G	Solvent
		ν	10^3K_ν	γ_H	$100K_{\gamma H}$	γ_G	$100K_{\gamma G}$	
hPDNB	35	0.705	8.11	0.567	1.10	0.564	1.46	THF
S. Deviation	0	0.007	0.72	0.002	0.03	0.003	0.07	THF
PCL-g-DAPE [34]	20	0.50	4.94	0.488	2.21			THF
PCL [41]	25	0.70	29					Benzene
aPP [36]	25	0.71	27					Toluene
PMA [23]	30	0.553	56.4					THF
PDiPF [28]	30	0.981	0.52					Toluene
35PDMPA [29]	30	0.555	4.82					Ethyl acetate

Table 2

Dimensional parameters for hPDNB in THF including K_θ, $(\overline{R}_0^2/\overline{M}_w)^{1/2}$, σ, C_∞ and B at 35 °C. polynorbornene (PNB), PCL-g-DAPE, PCL, aPP, PMA, and 35PDMPA are included for comparison.

Polymer	T (°C)	$100K_\theta$ (cgs)	10^{29} B (cgs)	$(\overline{R}_0^2/\overline{M}_w)^{1/2}$ Å	Σ	C∞	$(\overline{R}_{0f}^2/\overline{M}_w)^{1/2}$ Å	$(\overline{R}_{00}^2/\overline{M}_w)^{1/2}$ Å
hPDNB	35	8.32	56	0.675	1.98	7.86	0.341	0.241
S. Deviation		0.16	2	0.004	0.01	0.09		
PCL-g-DAPE [34]	20	5.09	0.01	0.573	2.18	9.53	0.263	0.186
PCL [41]	25	12.00	380	0.783	1.45	4.22	0.539	0.381
aPP [36]	25	16.60		0.835	1.76	6.19	0.475	0.336
PMA [23]	30	1.95	28.9	0.706	2.13	9.05	0.332	0.235
35PDMPA [29]	40	10.40	1.91	0.728	3.14	19.69	0.232	0.164

Table 3

Wormlike bead model characteristics of hPDNB and the characteristics values of 35PDMPA [29], poly(hydroxy ethers) PHE [27], and PDiPF [28] are listed for comparison.

Parameter	Low M_w	Eq (10)	35PDMPA	PHE	PDiPF
M_0 (g/mol)	408.7	408.7	176.2	284.0	100.1
$10^8 l$ (cm)	4.87	4.87	3.08	14.20	1.54
$10^{-8} M_L$ (cm)	83.9	83.9	57.2	20.0	65.0
10^{-} [23] $\Phi_{0,\infty}$	2.70	2.70	2.87	2.54	2.87
K_θ (cgs)	0.155	0.105	0.126	0.150	–
$10^{16}(<R_0^2>/M)$	0.692	0.534	0.579	0.690	–
$10^8 l_K$ (cm)	58.1	44.9	33.1	13.9	220
M_K	4873	3764	1895	278	29480
M_K/M_0	12	9	11	1	294
A_η	0.0	−10.7	−11.6		
A_0	0.00	−1.65	−2.11		–
d_{br}	0.54	0.73	0.60	0.54	–
$10^8 d_b$ (cm)	31.4	32.85	4.91	7.60	14
Σ	2.44	2.15	3.28	1.31	
C_∞	11.92	9.21	21.51	0.00	

by α which is the ratio of intrinsic viscosity of the polymeric chain in a good solvent [η] to the same in an ideal solvent $[\eta]_\theta$, and it was estimated by:

$$\alpha^3 = [\eta] \Big/ [\eta]_\theta = K_\theta \overline{M}_w^{1/2} \tag{6}$$

where K_θ was assessed from the Y-intercept of the S-F relationship, Eq (4). The values of α of hPDNB as shown in Fig. 5 were below 1.6 for all samples; therefore, equation (4) was applicable to the data.

Fig. 6 shows the plot of $[\eta]\,\overline{M}_w^{-1/2}$ against $\overline{M}_w^{1/2}$ according to S-F for hPDNB in THF at 35 °C. The value of K_θ was estimated by fitting a least-squares straight line to the experimental data. Table 2 shows the

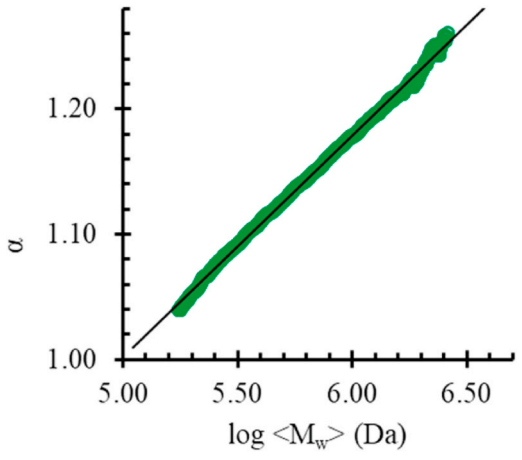

Fig. 5. Variations of calculated α values versus $<M_w>$ for hPDNB in THF at 35 °C.

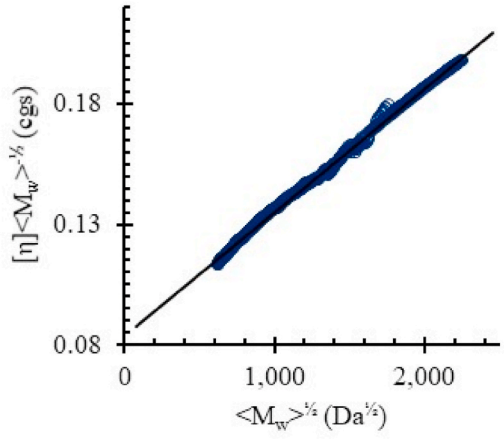

Fig. 6. Stockmayer-Fixman plots for hPDNB in THF at (—) 35 °C. The solid points show experimental data.

molecular parameters of hPDNB in the THF system, and the dimensional parameters of aPP, PMA, PCL, and PDPA, which are included for comparison.

The structure of hPDNB in THF at 30 °C was more compact than the other vinyl polymers. Because the value of $(\overline{R}_0^2/\overline{M}_w)^{1/2} = 0.675$ Å obtained for the fundamental conformational characteristic of hPDNB at 35 °C, was smaller than the end-to-end distance value obtained for flexible vinyl polymers and PCL, but larger than that of PCL-g-DAPE at θ temperature.

3.5. Evaluation of conformational characteristics

Flory characteristic ratio (C_∞) and steric factor (σ) were used to study the conformational characteristics of hPDNB in THF at 35 °C. The value of C_∞ relates to the freely jointed model whereas the mutual orientations of skeletal bonds are random and only bond lengths (l) are fixed. Therefore, it is the indication of the random-coil limit of the ratio of the unperturbed mean-square end-to-end distance of the real chain ($\overline{R}_0^2$) to a hypothetical freely joint random flight chain $\overline{R}_{00}^2 = nl$ [2]. It is showing restrictions on all directional correlations of skeletal bonds in the real chain and expressed in the form of [27,44–48].

$$C_\infty = \frac{lim\,\overline{R}_0^2}{\sum_i n_i l_i} = \overline{R}_0^2 \overline{R}_{00}^{-2} \tag{7}$$

The value $\overline{R}_{00}^2$ of hPDNB (last column of Table 2) was estimated by assuming the polymer chain units contain a rigid cyclopentane segment which is convenient to take as a virtual bond of length $(\overline{l}^2)^{1/2} = 2nl^2 \sim [2(n = 5)l_0^2]^{1/2} \sim 4.87$ Å. Thus, both conformational characteristics and rigidity factor may be uncertain as they depend on the choice of bonds and virtual bonds in the model chain [27]. The C_∞ value of hPDNB in

THF at 35 °C, obtained from Eq (7) ($C_\infty = 7.86 \pm 0.10$), is also tabulated in the 7th column of Table 2. The value of C_∞ does not describe the rigidity of the hPDNB since this value is in the range of C_∞ of atactic flexible vinyl polymers with aliphatic side chains, which are in the range of $5 < C_\infty < 10$ [49]. The value of C_∞ of acrylic polymers with bulky side groups, such as poly(3,5-dimethyl phenyl acrylate) (35PDMPA) in ethyl acetate (EA), was found to be about 18.5–18.9 which is considerably higher than flexible acrylic polymers.

Another parameter to characterize conformational rigidity of the polymer chains in solution is the rigidity factor, σ, (Eq (8)) which reflects the effect of a hindrance to free rotation of a bond around the main chain, defined as:

$$\sigma = \left(\overline{R}_0^{\,2}\overline{R}_{0f}^{\,-2}\right)^{1/2} \tag{8}$$

The $\overline{R}_{0f}^{\,2}$reflects the mean square end-to-end dimension of a freely rotating hypothetical polymeric chain in which the bond length (l) and bond angle (ϕ) are restricted. In this case, the mean-square end-to-end distance expressed by Eq. (9) [44].

$$\overline{R}_{0f}^{\,2} = nl^2\frac{(1 - Cos\,\phi)}{(1 + Cos\,\phi)} = 2nl^2 \tag{9}$$

The $\overline{R}_{0f}^{\,2}$ value of hPDNB was obtained experimentally from the Y-intercept of the S-F relationship (Eq (4)). Then the values of $\sigma = 1.98 \pm 0.01$ for hPDNB in THF were evaluated by Eq (8) and are tabulated in the 6th column of Table 2 along with the same values for PCL, PCL-g-DAPE, and a few (meth)acrylic polymers for comparison. The low σ value of hPDNB in THF compared to the other vinyl polymers reflects the effective free rotation of the main chain. Therefore, the effects of the bulky rosin side groups did not induce a very large restriction to the free rotation of the main chain. Though the σ values of hPDNB were lower than the σ value of PMA, it falls in the range of the σ values found for acrylic flexible polymers ($1.5 < \sigma < 2.5$). For more rigid acrylic polymers such as 35PDMPA, the σ value is around 3 due to the hindrance effects induced by the preferred orientation of lateral groups about the orientation of the polymer backbone.

Low values of C_∞ and σ suggest rather high flexibility of the hPDNB chains. This may be surprising given the presence of a 1,3-cyclopentane ring in the main chain repeating unit with a bulky rosin group. In general, rigid and long units in the main chains such as 1,3-cyclopentane in hPDNB and C–Ph–O in polycarbonates [44] or –C–Ph–NH in polyurethanes [45] can exert two opposing effects on the spatial configuration of the chain. Due to their length and stiffness, they make the chain more extended. The extended chain has less spatial interaction between groups separated by three or more skeletal bonds and the net result is a low value of the conformational parameters.

4. Wormlike touched-bead

In the previous section, we observed that a random flight chain model could not describe the behavior of hPDNB, satisfactorily. This section attempts to characterize the polymer by the theory of the wormlike touched-bead model [27,44–47]. and compare the results with previous sections. According to this theory, the interpretation of the intrinsic viscosity of hPDNB in THF requires estimation of three characteristic parameters: cross-sectional chain diameter expressed as A_η (Eq (11)), the flexibility of the chain coming from K_θ (Eq (5) and Eq (8)), and polymer-solvent interaction associated with B (Eq (13)) by z (Eq (14)). Based on this theory, the intrinsic viscosity at theta conditions depends not only on the $\overline{R}_0^{\,2}$ but also on the cross-sectional dimensions of the polymer, called the diameter of the bead (d_b), with the beads being the smallest units that compose the conformation of the macromolecule in solution. The results of the theory have been expressed in a simple form convenient for use, even with very short chains, by Bohdanecký [24,27,47].

$$[\eta] = \left(A_\eta + K_\theta \overline{M}_w^{1/2}\right)\left[1 + \left(\frac{3}{4}\right)\left(\frac{3}{2\pi}\right)^{3/2} K(n_K) C_{\eta(\infty)} B \left(\frac{\overline{R}_0^{\,2}}{\overline{M}_w}\right)_\infty^{-\frac{3}{2}} \overline{M}_w^{1/2}\right] \tag{10A}$$

which after r earranging yields [29]:

$$[\eta] = A_\eta + \left[\left(\frac{3}{4}\right)\left(\frac{3}{2\pi}\right)^{3/2} A_\eta \left(\frac{<R_0^2>}{\overline{M}_w}\right)_\infty^{-\frac{3}{2}} K(n_K) C_\eta B + K_\theta\right]\overline{M}_w^{1/2} + \left(\frac{3}{4}\right)\left(\frac{3}{2\pi}\right)^{3/2} K_\theta \left(\frac{<R_0^2>}{\overline{M}_w}\right)_\infty^{-\frac{3}{2}} C_\eta K(n_K) B \overline{M}_w \tag{10B}$$

With:

$$\left(\frac{\overline{R}_0^2}{\overline{M}_w}\right)_\infty = \frac{l_K}{M_L} \tag{11}$$

$$M_k = l_k M_L \tag{12}$$

$$A_\eta = K_\theta A_0 (d_{br}) M_{K^{1/2}} \tag{13}$$

$$d_{br} = d_b / l_K \tag{14}$$

$$A_0 = -2.9 + 5.36 d_{br}\ when^{47} 0.3 \le d_{br} \le 0.8 \tag{15}$$

$$\log d_r = -0.1374 A_0^2 - 0.5001 A_0 - 0.4488.\ for\ dr\ larger\ than\ 0.1 \tag{15B}$$

$$K_\theta = \varphi_{0,\infty}\left(\overline{R}_0^2 \overline{M}_w^{-1}\right)_\infty^{3/2} \tag{16}$$

The functionality of $K(n_K)$ was derived by Yamakawa and Shimada [48,50]. The constants of Eq (15) do not have specific meanings; their function is to relate A_0 to d_{br}. $(\overline{R}_0^{\,2}\overline{M}_w^{\,-1})_\infty$ is the ratio of $\overline{R}_0^{\,2}$ and $\overline{M}_w$ in the random coil limit where $\overline{M}_w \to \infty$, and $\Phi_{0,\infty} = 2.87 \times 10^{23}$ (cgs) is the Flory constant where $\overline{M}_w \to \infty$. Therefore, K_θ in (Eq (10)) has the same meaning as K_{MH} (Eq (1)) in a theta solvent when $M \to \infty$. A_0 is a function of the reduced bead diameter, d_{br} (Eq (14)). M_L is the shift factor which is usually set equal to the molecular weight per unit contour length of the chain at full length; l_K and M_K are the length and molecular weight of the Kuhn statistical segment, respectively. The cylinder and touched-bead theories reduce to the Einstein equation for rigid spheres at $L = d = d_b$ and are identical.[47]

Eq (10B) has the quadratic form of $y = ax$ [2] $+ bx + c$. Therefore, adjustment of a quadratic polynomial to [η] and $\overline{M}_w^{1/2}$ data yields the exact solution for Eq (10B). Fig. 7 shows the downward second-degree polynomial curves fitted onto [η] vs $\overline{M}_w^{1/2}$ data of hPDNB-THF systems at 35 °C. Equation (10C) represses the variation of all the [η] and $\overline{M}_w^{1/2}$ data of the hPDNB-THF at 35 °C:

$$[\eta] = 4.5207\ \mathrm{X}\ 10^{-5}\overline{M}_W + 0.10091\overline{M}_w^{1/2} - 10.703 \tag{10C}$$

By comparing Eq (10B) with Eq (10C) the coefficients of Eq (10B) for hPDNB in THF at 35 °C are:

$$A_\eta = -.10.7_{03} \tag{18A}$$

$$(3/4) A_\eta C_{\eta\,\infty}\left(\frac{3}{2\pi}\right)^{\frac{3}{2}}\left(\frac{<R_0^2>}{\overline{M}_w}\right)_\infty^{-\frac{3}{2}} K(n_K) B + K_\theta = 0.10091 \tag{18B}$$

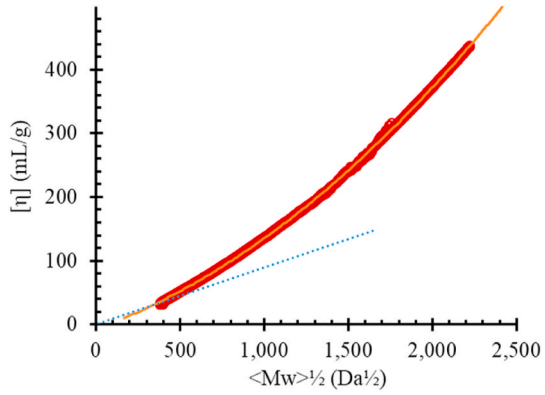

Fig. 7. Variation of [η] versus $\overline{M}_w^{1/2}$ based on touched bead model for hPDNB in THF at (—) 35 °C. The solid points show experimental data.

$$(¾)K_\theta C_\eta \infty \left(\frac{3}{2\pi}\right)^{\frac{3}{2}} \left(\frac{< R_0^2 >}{\overline{M}_w}\right)_\infty^{-\frac{3}{2}} K(n_K)B = 4.5207X10^{-5} \quad (18C)$$

.The characteristic parameters of hPDNB at 35 °C obtained from the above polynomial are tabulated in Table 3 along with the same parameters for other polymers for comparison. The value of K_θ calculated from polynomial adjustment is about 22% higher than the values obtained from the SF method (Table 2 column 3).

The higher values of the obtained K_θ by applications of Eq (10B), represented as (10C), is proof that the chain stiffness contributed to the slope of the SF plot; therefore, the values of K_θ were underestimated by the SF extrapolations to M → 0 using the SF plot. The intrinsic viscosity of polymers in solution does not depend strongly on the diameter of the chain, however, the obtained value for the diameter of hPDNB (33 Å) is near to the calculated diameter of the repetitive units of hPDNB using a molecular model (35 Å). As shown in Table 3, the molecular weight of the Kuhn statistical segment, M_K, of hPDNB is 9 times higher than the molecular weight of its repeating unit; somehow similar to 35PDMPA in EA at 30 °C, which was 11 times higher than its M_0, the molar mass of its mer. This indicates that hPDNB in THF behaves as semi-rigid polymers similarly to 35PDMPA in EA. The values of C_∞ and σ were evaluated by S-F method of 7.9 and 1.98, respectively; however, these values do not refer to a rigid polymer. The values of l_K, and M_K of hPDNB were not as low as the ones of bisphenol-A based poly(hydroxyethers) (PHE) [27], a very flexible polymer, neither were they as high as the ones for poly (diisopropyl fumarate) (PDiPF) [28], a semi-rigid polymer, but they were higher than of the 35PDMPA. Therefore, the worm-like touch-bead model describes better the solution properties of the hPDNB in THF at 35 °C.

5. Conclusions and remarks

Online size exclusion chromatography with two-angle light scattering and differential pressure viscosity was used to characterize a sample of rosin substituted hydrogenated polynorbornene (hPDNB) in THF at 35 °C. The characteristic parameters of the polymer in THF such as MH's parameters, the hydrodynamic radii, and refractive index increment, and end-to-end dimensions were found to be in the range of the values for flexible polymers. The polymer was described better by the touched-bead model that indicated the polymer is more rigid than PMA, a random flexible macromolecule, and more flexible than PDiPF, a hindered rigid macromolecule.

Funding

The National Science Foundation (DMR-1252611) supported this synthesis work. The U.S. Department of Agriculture, National Institute of Food and Agriculture, Evans-Allen project number SCX-311-29-21 and SCX-311-21-17 supported solution behavior investigation.

Data availability

The raw and processed data required to reproduce these findings are available upon request nhamidi@scsu.edu.

CRediT authorship contribution statement

Nasrollah Hamidi: Conceptualization, Methodology, Software, Validation, Data curation, Writing – original draft, Visualization, Investigation, Writing – review & editing. **Mitra Shiran Ganewatta:** Polymer synthesis, Conceptualization, Validation, Data curation, Visualization, Investigation, Writing – review & editing.

Declaration of competing interest

The authors declare that they have no known competing financial interests or personal relationships that could have appeared to influence the work reported in this paper.

Acknowledgments

The authors acknowledge Prof. Chuanbing Tang (University of South Carolina) for granting the use of the sample polymer. The authors declare no competing financial interest. In addition, NH is grateful for the supports of Judith Sally, and Louis Whitesides.

References

[1] Z. Wang, M.S. Ganewatta, C. Tang, Sustainable polymers from biomass: bridging chemistry with materials and processing, Prog. Polym. Sci. 101 (2020) 101197.
[2] J. Bohlmann, C.I. Keeling, Terpenoid biomaterials, Plant J 54 (2008) 656–669.
[3] J. Wang, K. Yao, A.L. Korich, S. Li, S. Ma, et al., Combining renewable gum rosin and lignin: towards hydrophobic polymer composites by controlled polymerization, J. Polym. Sci., Part A: Polym. Chem. 49 (2011) 3728–3738.
[4] S. Kugler, P. Ossowicz, K. Malarczyk-Matusiak, E. Wierzbicka, Advances in rosin-based chemicals: the latest recipes, applications and future trends, Molecules 24 (2019) 1651.
[5] P.A. Wilbon, F. Chu, C. Tang, Progress in renewable polymers from natural terpenes, terpenoids, and rosin, Macromol. Rapid Commun. 34 (2013) 8–37.
[6] K. Yao, C. Tang, Controlled polymerization of next-generation renewable monomers and beyond, Macromolecules 46 (2013) 1689–1712.
[7] Y. Zheng, K. Yao, J. Lee, D. Chandler, J. Wang, et al., Well-defined renewable polymers derived from gum rosin, Macromolecules 43 (2010) 5922–5924.
[8] P.A. Wilbon, Y. Zheng, K. Yao, C. Tang, Renewable rosin acid-degradable caprolactone block copolymers by atom transfer radical polymerization and ring-opening polymerization, Macromolecules 43 (2010) 8747–8754.
[9] K. Yao, J. Wang, W. Zhang, J.S. Lee, C. Wang, et al., Degradable rosin-ester–caprolactone graft copolymers, Biomacromolecules 12 (2011) 2171–2177.
[10] Y. Liu, K. Yao, X. Chen, J. Wang, Z. Wang, et al., Sustainable thermoplastic elastomers derived from renewable cellulose, rosin and fatty acids, Polym. Chem. 5 (2014) 3170–3181.
[11] Y. Chen, P.A. Wilbon, J. Zhou, M. Nagarkatti, C. Wang, et al., Multifunctional self-fluorescent polymer nanogels for label-free imaging and drug delivery, Chem. Commun. 49 (2013) 297–299.
[12] J. Wang, Y.P. Chen, K. Yao, P.A. Wilbon, W. Zhang, et al., Robust antimicrobial compounds and polymers derived from natural resin acids, Chem. Commun. 48 (2012) 916–918.
[13] M.S. Ganewatta, Y.P. Chen, J. Wang, J. Zhou, J. Ebalunode, et al., Bio-inspired resin acid-derived materials as anti-bacterial resistance agents with unexpected activities, Chem. Sci. 5 (2014) 2011–2016.
[14] M.S. Ganewatta, K.P. Miller, S.P. Singleton, P. Mehrpouya-Bahrami, Y.P. Chen, et al., Antibacterial and biofilm-disrupting coatings from resin acid-derived materials, Biomacromolecules 16 (2015) 3336–3344.
[15] M.S. Ganewatta, W. Ding, M.A. Rahman, L. Yuan, Z. Wang, et al., Biobased plastics and elastomers from renewable rosin via "living" ring-opening metathesis polymerization, Macromolecules 49 (2016) 7155–7164.
[16] M.A. Rahman, H.N. Lokupitiya, M.S. Ganewatta, L. Yuan, M. Stefik, et al., Designing block copolymer architectures toward tough bioplastics from natural rosin, Macromolecules 50 (2017) 2069–2077.
[17] P.J. Flory, M. Volkenstein, Statistical Mechanics of Chain Molecules, Wiley Online Library, 1969.
[18] Z. Xu, N. Hadjichristidis, L.J. Fetters, Solution properties and chain dimensions of poly (n-alkyl methacrylates), Macromolecules 17 (1984) 2303–2306.

[19] L. Gargallo, N. Hamidi, D. Radic, Synthesis, solution properties and chain flexibility of poly (2, 6-dimethylphenyl methacrylate), Polymer 31 (1990) 924–927.
[20] L. Yuan, N. Hamidi, S. Smith, F. Clemons, A. Hamidi, et al., Molecular characterization of biodegradable natural resin acid-substituted polycaprolactone, Eur. Polym. J. 62 (2015) 43–50.
[21] W.H. Stockmayer, M. Fixman, On the estimation of unperturbed dimensions from intrinsic viscositiesxcin, J. Polym. Sci., Part C: Polym. Symp. 1 (1963) 137–141.
[22] Y. Abe, P. Flory, Configurational statistics of 1, 4-polybutadiene chains, Macromolecules 4 (1971) 219–229.
[23] H. Ikeda, H. Shima, Solution properties of polymethyl acrylate I. Properties of PMA chain by viscometric method, Eur. Polym. J. 40 (2004) 1565–1574.
[24] M. Bohdanecky, New method for estimating the parameters of the wormlike chain model from the intrinsic viscosity of stiff-chain polymers, Macromolecules 16 (1983) 1483–1492.
[25] H. Yamakawa, M. Fujii, Intrinsic viscosity of wormlike chains. Determination of the shift factor, Macromolecules 7 (1974) 128–135.
[26] Y. Fujii, Y. Tamai, T. Konishi, H. Yamakawa, Intrinsic viscosity of oligo-and poly (methyl methacrylate)s, Macromolecules 24 (1991) 1608–1614.
[27] A. Kaštánek, S. Podzimek, J. Dostál, L. Šimek, M. Bohdanecký, Estimation of conformational characteristics of bisphenol-A based poly (hydroxyethers), Polymer 41 (2000) 2865–2870.
[28] A. Matsumoto, E. Nakagawa, Evaluation of chain rigidity of poly (diisopropyl fumarate) from light scattering and viscosity in tetrahydrofuran, Eur. Polym. J. 35 (1999) 2107–2113.
[29] N. Hamidi, T. Best, Characteristics of poly (3,5-dimethylphenylacrylate) in ethyl acetate at 25 and 30 C, J. Macromol. Sci. Part B Phys. 53 (2014) 931–955.
[30] F. Blank, C. Janiak, Metal catalysts for the vinyl/addition polymerization of norbornene, Coord. Chem. Rev. 253 (2009) 827–861.
[31] J.P. Klein, R.A. Register, Tuning the phase behavior of semicrystalline hydrogenated polynorbornene via epimerization, J. Polym. Sci., Part B: Polym. Phys. 57 (2019) 1188–1195.
[32] D. Lecacheux, J. Lesec, Measurement of the dead volume between concurrent detectors in gel permeation chromatography, J. Liq. Chromatogr. 5 (1982) 2227–2239.
[33] K. Terao, J.W. Mays, On-line measurement of molecular weight and radius of gyration of polystyrene in a good solvent and in a theta solvent measured with a two-angle light scattering detector, Eur. Polym. J. 40 (2004) 1623–1627.
[34] N. Hamidi, S. Edmonds, V. Frazier, F. Clemons, Temperature dependence characteristics of biodegradable polycaprolactone grafted propargyl dehydroabietic ester (PCL-g-DAPE), J. Macromol. Sci. Part B Phys. 57 (2018) 129–150.
[35] J. Li, S. Harville, J.W. Mays, Second virial coefficients and radii of gyration for poly (α-methylstyrene) in cyclohexane below the ϑ temperature, Macromolecules 30 (1997) 466–469.
[36] J. Brandrup, E.H. Immergut, E.A. Grulke, A. Abe, D.R. Bloch, Polymer Handbook, vol. 89, Wiley, New York, 1999.
[37] H. Yamakawa, Modern Theory of Polymer Solutions, Harper & Row, 1971.
[38] H. Morawetz, Macromolecules in Solution, Interscience Publishers, New York, 1965, p. 21.
[39] D. Yoon, P. Sundararajan, P. Flory, Conformational characteristics of polystyrene, Macromolecules 8 (1975) 776–783.
[40] E. Temyanko, P.S. Russo, H. Ricks, Study of rodlike homopolypeptides by gel permeation chromatography with light scattering detection: validity of universal calibration and stiffness assessment, Macromolecules 34 (2001) 582–586.
[41] M.A. Woodruff, D.W. Hutmacher, The return of a forgotten polymer—polycaprolactone in the 21st century, Prog. Polym. Sci. 35 (2010) 1217–1256.
[42] R. Mendichi, L. Šoltés, A. Giacometti Schieroni, Evaluation of radius of gyration and intrinsic viscosity molar mass dependence and stiffness of hyaluronan, Biomacromolecules 4 (2003) 1805–1810.
[43] P.J. Flory, Principles of Polymer Chemistry, Cornell University Press, 1953 (p Chapter XIV).
[44] A. Williams, P.J. Flory, Configurational statistics of poly (ethylene terephthalate) chains, J. Polym. Sci. 2 Polym. Phys. 5 (1967) 417–424.
[45] V. Kašpárková, L. Šimek, M. Bohdanecký, Estimation of the conformational characteristics of polyurethane chains, Macromol. Chem. Phys. 197 (1996) 3757–3772.
[46] T. Yoshizaki, I. Nitta, H. Yamakawa, Transport coefficients of helical wormlike chains. 4. Intrinsic viscosity of the touched-bead model, Macromolecules 21 (1988) 165–171.
[47] M. Bohdanecký, M. Netopilík, Note on the application of the Yoshizaki-Nitta-Yamakawa theory of the intrinsic viscosity of the touched-bead model, Makromol. Chem. Rapid Commun. 14 (1993) 383–386.
[48] H. Yamakawa, J. Shimada, Stiffness and excluded-volume effects in polymer chains, J. Chem. Phys. 83 (1985) 2607–2611.
[49] J.M.G. Cowie, V. Arrighi, Polymers: Chemistry and Physics of Modern Materials, CRC press, 2007.
[50] J. Shimada, H. Yamakawa, Statistical mechanics of helical wormlike chains. XII. Multivariate distribution functions, J. Chem. Phys. 73 (1980) 4037–4044.